Solar Extreme Ultraviolet Variability of the X-class Flare on April 21, 2002 and the Terrestrial Photoelectron Response

Thomas N. Woods[1], Scott M. Bailey[2], W. K. Peterson[1], Stanley C. Solomon[4], Harry P. Warren[3], Francis G. Eparvier[1], Howard Garcia[5], Charles W. Carlson[6], and James P. McFadden[6]

[1]*Laboratory for Atmospheric and Space Physics, University of Colorado, Boulder, Colorado.*
[2]*Geophysical Institute, University of Alaska, Fairbanks, Alaska*
[3]*Naval Research Laboratory, Washington, DC*
[4]*High Altitude Observatory, National Center for Atmospheric Research, Boulder, Colorado*
[5]*NOAA Space Environment Center, Boulder, Colorado*
[6]*University of California, Berkeley, California*

The near-simultaneous observations of the solar extreme ultraviolet (EUV) irradiance and terrestrial photoelectron distribution during and after the X-class flare on April 21, 2002 provide for a distinctive study of the effects that a solar flare can have on Earth's upper atmosphere. The solar EUV irradiance from 0.1-195 nm was measured by the Solar EUV Experiment (SEE) aboard the NASA Thermosphere, Ionosphere, Mesosphere, Energetics, and Dynamics (TIMED) satellite. The terrestrial photoelectron distribution from 10-1000 eV was measured by the Fast Auroral Snapshot (FAST) energetic electron sensor. The variations of the solar EUV irradiance from the X-class flare at ~2 UT on April 21, 2002 range from more than a factor of 10 for the X-ray emissions to less than 10% at longer EUV wavelengths. The measured ratio of the flare spectrum to the pre-flare spectrum has a spectral shape that is similar to that predicted for the Bastille Day 2000 flare. Most of the solar irradiance variation is in the X-ray range and is due to coronal emissions. The photoelectron distribution changed by a factor of about 10 for the high-energy Auger electrons and by very little for the low-energy electrons. Modeling the photoelectron distribution using the measured solar EUV irradiance provides results that are qualitatively consistent with the observed photoelectron distribution. This study is focused primarily on the relative changes during the flare compared to the pre-flare conditions.

INTRODUCTION

There are, on average, one modest M-class solar flare every two days and one large X-class flare per month as determined from a survey of flares during solar cycles 21 and 22 [*Garcia*, 2000]. Of course, there are more flares during solar maximum conditions than at solar minimum. Most of these flares affect the solar irradiance only in the X-ray region, but sometimes a large flare can affect the solar irradiance over a broad wavelength range up to 180 nm [e.g., *Brekke et al.*, 1996; *Meier et al.*, 2002; *Woods et al.*, 2003]. Flare events and the associated abrupt changes to Earth's upper atmosphere are an important aspect of space weather studies that are relevant to space-based communication/navigation systems and astronaut safety. Measurement of the solar EUV irradiance is needed on time scales of seconds to hours to improve the understanding of how flares cause abrupt space weather changes (*e.g.* sudden ionospheric disturbances or SIDs). This study examines solar EUV and soft X-ray irradiance variations during the large X1.5 flare on 21 April 2003, and the photoelectron response to this flare, as a step toward understanding some of the effects that flares can have on Earth's upper atmosphere.

An attempt has been made to model the increase in the EUV spectral irradiance during the Bastille Day 2000 flare [Meier *et al.,* 2002]. According to this model the increase in EUV irradiance during the flare was comparable in magnitude to the solar cycle increase, but there are large differences in the spectral shape between the flare variations and the solar cycle variations. The TIMED SEE instrument has several measurements of large flares over the full EUV spectral range available for comparison to flare models. However, this initial study is focused on the 21 April 2002 flare event.

Instrumentation on the FAST satellite [*Carlson et al.*, 2001] observed upward flowing photoelectrons over the energy range 10 to 1000 eV at nearly the same time as the SEE solar measurements. Photoelectrons are those electrons produced in the upper atmosphere through photoionization by solar radiation (primary photoelectrons), as well as, through secondary ionization by other energetic photoelectrons (secondary photoelectrons). The photoelectron energy spectrum is very sensitive to the magnitude and wavelength distribution of the solar EUV irradiance, so the observed photoelectrons are a good tracer of energy deposition from the solar flare. These near-simultaneous measurements of the solar EUV irradiance and photoelectrons can provide validation for photoelectron models.

SOLAR MEASUREMENTS

The TIMED SEE consists of two instruments to measure the solar vacuum ultraviolet (VUV) spectral irradiance from 0.1 to 195 nm [*Woods et al.*, 1998]. The EUV Grating Spectrograph (EGS) is a normal incidence Rowland circle spectrograph that has a spectral range of 26 to 195 nm with 0.4 nm spectral resolution. The EGS photon-counting detector is a CODACON array detector (64 x 1024 anodes) that uses microchannel plates (MCP) and coded anode electronics for its readout. The XUV Photometer System (XPS) includes nine silicon XUV photodiodes with thin film filters deposited directly on the photodiode. This XUV photometer set measures the solar irradiance from 0.1 to 34 nm with each filter having a spectral bandpass of about 7 nm. Observations by similar solar XUV photometers flown on sub-orbital vehicles and on the Student Nitric Oxide Explorer (SNOE) satellite are described by *Bailey et al.* [2000; 2001]. The pre-flight accuracy of the SEE instruments is about 10% as derived from calibrations of XPS and EGS with synchrotron radiometric sources [*Woods et al.*, 1999; *Eparvier et al.*, 2001]. Using redundant channels and rocket underflight calibrations to track in-flight changes to the instrument, the accuracy of the SEE solar measurements is about 15%.

The TIMED spacecraft was launched in December 2001, and daily measurements of the solar VUV irradiance by SEE began on 22 January 2002. Because of the configuration of SEE on the TIMED spacecraft, the SEE solar observations are limited to about 3 minutes per orbit, with the TIMED orbital period being about 97 minutes. During these 3-minute observations, SEE normally obtains 18 integrations, each of 10 s duration, while the sun moves through the instruments' ~12° field of view. Although SEE was not designed to study flares, as can be seen from its low duty cycle for the solar observations, the XPS has observed several flares in its X-ray channels. With the large X-class flare on 21 April 2002, both the XPS and EGS recorded significant increases near the peak of the flare event and a slow decay over several hours. As shown in Figure 1, the time series of the SEE observations of this flare event are consistent with the high time resolution X-ray observations made by the GOES X-Ray Sensor (XRS) [*Garcia*, 1994].

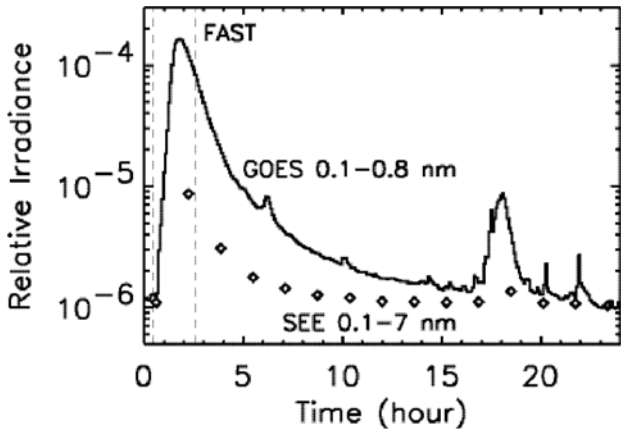

FIGURE 1: Time Series of SEE and GOES solar X-ray measurements on April 21, 2002. The SEE measurements (diamond symbols) at 0:36 and 2:14 UT are the focus here because the FAST photoelectron measurements (indicated by the vertical dashed lines) were at 0:26 and 2:33 UT.

This flare near the solar west limb was imaged by the Transition Region And Coronal Explorer (TRACE) instrument, as shown in Figure 2. TRACE is a multi-layer imaging telescope capable of making observations in several relatively narrow wavelength bands [*Handy et al.*, 1999]. The TRACE 19.5 nm bandpass is particularly useful for flare observations since it images the Fe XXIV 19.2 nm emission, in addition to the cooler Fe XII 19.5 nm emission. The TRACE observations indicate that this flare was a two-ribbon, long duration event similar to the 2000 Bastille day flare studied by *Meier et al.* [2002]. Additional observations are available from the instruments aboard the Solar and Heliospheric Observatory (SOHO).

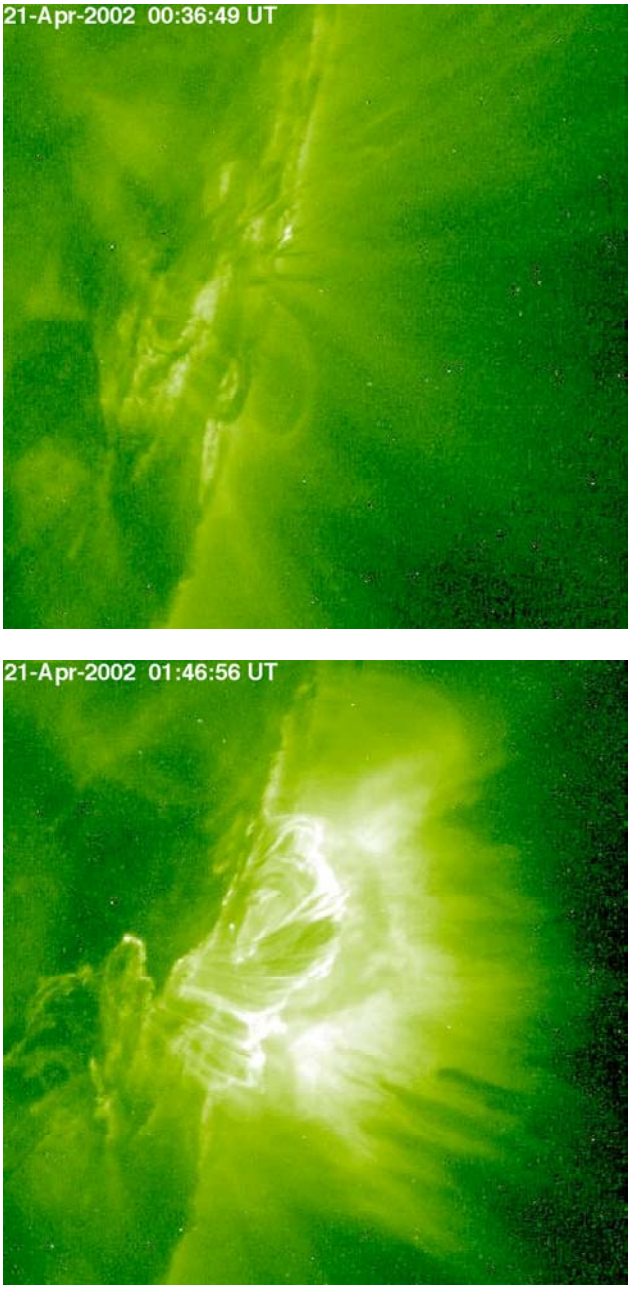

FIGURE 2. TRACE 19.5 nm image of the X-class flare on April 21, 2002. The top image is taken at 0:37 (pre-flare). The emission in this image is due mainly to Fe XII (19.5 nm) formed at 1.5 MK. The bottom image is at 1:47 (flare peak). During this time a diffuse component also becomes visible which is due to Fe XXIV (19.2 nm) that is formed at 15-20 MK.

Solar irradiance measurements, provided by SEE from 0.1 to 195 nm, are critical for accurately modeling the photoelectron response to the solar flare. The ratio of the flare irradiance spectrum to the pre-flare spectrum clarifies which spectral features increased during the flare event. This ratio, shown in Figure 3, is more than a factor of 8 in

the X-ray region measured by the XPS and is less than a factor of 2 for the EUV region measured by the EGS. The EGS flare spectrum shows much smaller variations than the X-ray variations, as expected, and shows that the EUV variations are primarily from coronal emissions. It appears that this flare had little, if any, effect on the solar irradiance longward of 170 nm.

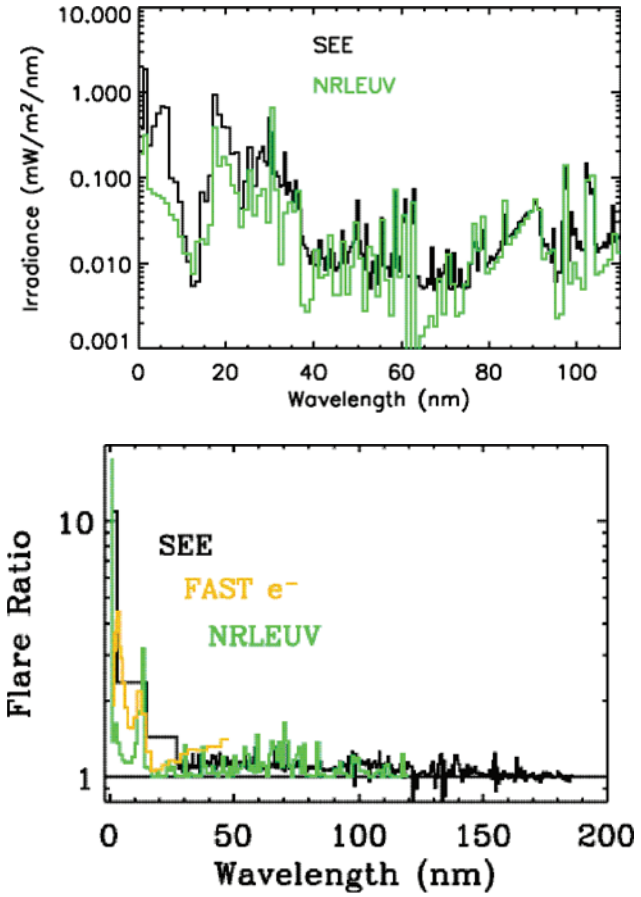

FIGURE 3. Flare and pre-flare solar irradiance. The flare solar irradiance from the SEE measurements and predictions from the NRLEUV model of the Bastille Day 2002 flare are given in the top plot. The ratio of the flare spectrum to pre-flare spectrum is given in the bottom plot. The SEE XPS and EGS data are used shortward and longward of 27 nm, respectively. The ratio of the FAST photoelectron distribution is also shown in the bottom plot as a first order approximation of the solar irradiance increase. The wavelength for the photoelectron ratio is calculated after making a correction of 20 eV for the average ionization potential.

All of the XUV photometers are sensitive to X-rays shortward of 7 nm, so a special correction is needed for the XPS longer-wavelength channels (17-34 nm). The XPS signals are first corrected using the XPS 0-7 nm channel (Ti-coated photodiode) before calculating the 17-34 nm irradiance. This correction is small for non-flare XPS data

but is large for flare data. Consequently, the uncertainty for XPS flare data is larger than for non-flare data. An additional approach was also employed to explore the short-wavelength sensitivity of the XUV photometers, comparing XPS flare and pre-flare data to deduce the increase of the solar radiation over a limited spectral range. Using a least-squared fitting algorithm and the various bandpasses of the individual channels, a peak near 2 nm was found for the flare irradiance, which is consistent with the flare model and photoelectron measurements as described below.

SOLAR FLARE MODELING

The NRLEUV model [*Warren et al.,* 2001] uses emission measure techniques together with radiative transfer and solar image decomposition to predict the solar EUV irradiance. A special example of the NRLEUV model is the prediction of the solar EUV irradiance for the Bastille Day 2000 flare [*Meier et al*., 2002]. The NRLEUV model cannot make predictions for the April 21 flare due to the lack of solar radiance measurements needed to generate the temperature profile in the solar atmosphere for the April 21 flare. Therefore, the Bastille Day 2000 flare model is used for comparing to the SEE flare measurements. With the Bastille Day flare having a X-class rating 4 times higher than the April 21 flare rating, the ratio of the NRLEUV flare spectrum to the pre-flare spectrum [*Meier et al*., 2002] is scaled down by a factor of 4, shown as the green spectrum in Figure 3. These irradiance values are consistent with the SEE measurements longward of 27 nm, but the NRLEUV irradiances are lower than the SEE measurements shortward of 27 nm by about a factor of 2 near 17 nm. The focus here is on the relative change of the solar EUV irradiance during the flare event, so the validation of the SEE measurements will be presented in a future publication.

The relative change predicted by the NRLEUV model is similar to the ratio of the flare spectrum to the pre-flare spectrum that is determined from the SEE measurements. The flare ratios in the EUV range are consistent, whereas the XUV changes measured by SEE XPS are higher than the NRLEUV predictions at most wavelengths. This difference is partially related to the broadband nature of the XPS measurements, which are being compared to the higher resolution NRLEUV model predictions. In addition, the XPS measurements longward of 7 nm are contaminated during a flare event by the largest increase occurring in the X-ray region, where the XUV photodiodes have good sensitivity. While a correction for the X-ray contribution is applied as part of the XPS data processing algorithm, the X-ray correction reduces the uncertainties for the XPS measurements, especially for flare data when the X-ray contribution is large.

PHOTOELECTRON MEASUREMENTS

Photoelectron spectra were measured during two 2-minute intervals on 21 April 2002, centered on the times indicated in Figure 1. The data were obtained from the FAST array of electron detectors [*Carlson et al.*, 2001]. The two measurements are plotted in Figure 4. At the times of observation, FAST was at an altitude of ~3700 km, in the southern hemisphere with the solar zenith angle at the foot of the field lines near 87° for each observation. Upward-flowing fluxes were observed within 20° of the magnetic field direction. The data intervals were selected to be well equatorward of precipitating auroral electrons, and away from the peak of the outer radiation belt region and its associated penetrating radiation environment. These high altitude photoelectrons have an energy distribution above ~20 eV that is similar to the energy distribution of the source population in the thermosphere (100-400 km) because of the low collisional frequency above 400 km and the lack of other sources for higher energy electrons away from the polar regions [e.g., *Oran and Strickland*, 1978]. Modeling of the photoelectron spectrum generation and propagation out of the atmosphere is discussed in the following section.

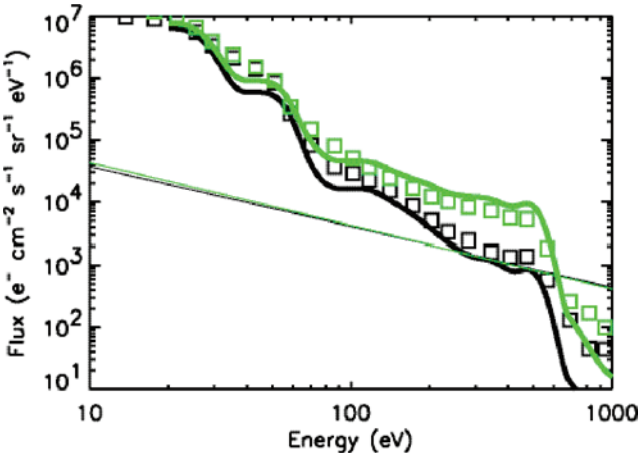

FIGURE 4. Photoelectron distribution from FAST measurements and GLOW model results. The boxes are the FAST observations. The straight, thin lines are the backgrounds, which have been subtracted. The thick lines are results from the GLOW photoelectron model. Black color represents the time period just before the solar flare. Green represents the time period during the solar flare.

Spacecraft generated photoelectrons are observed near 90° pitch angle and so are not included in the spectra shown in Figure 4. In addition, a small background signal is present that has been subtracted from the data. The background level is estimated assuming that there were no photoelectrons with energies above 5000 eV. The energy dependence of the background calculated this way is consistent with the inverse energy dependence of a background flux expected

from the instrumental geometry. The color-coded straight lines on Figure 4 indicate the photoelectron flux equivalent of this background. The background fluxes are significantly lower than the net reported fluxes for most of the energy range displayed in Figure 4, up to ~600 eV.

Photoelectron fluxes have been measured at significantly higher energy resolution by Doering and his colleagues than that reported here from the FAST satellite. These higher resolution measurements were made both within the collision dominated ionospheric production region [e.g., *Lee et al.,* 1980] and in the collisionless region above [e.g. *Peterson et al.* 1977]. Signal to noise considerations limited the Doering group's observations of photoelectrons to energies below ~80 eV. *Winningham et al.* [1989] extended the energy range to several hundred eV using data from DE-2. The FAST measurements extend the energy range for the photoelectron flux to about 1000 eV.

The FAST electron detectors are sensitive to Auger photoelectrons in the 100 to 1000 eV range. The high sensitivity was obtained by careful design, multiple sensors, avoidance of the known sources of noise from spacecraft, and averaging over long two-minute intervals. Auger electrons are those photoelectrons produced through K-shell photoionization. Auger effects are known to have an important effect on photoelectron spectra in the > 300 eV range [*Winningham et al.*, 1989]. The data presented in Figure 4 clearly demonstrate that the high sensitivity and background rejection of the FAST electron spectrometers allow routine detection of photoelectron generation up to ~600 eV. The pre-flare photoelectron FAST observations agree well in magnitude and shape with the photoelectron spectra analyzed by *Winningham et al.* [1989]. The FAST electron detectors have been routinely operating to acquire photoelectron spectra since February 1999. We will describe these observations, obtained over a range of solar activity, in a future publication.

The ratio of the flare and pre-flare photoelectron distribution provides an estimate of the solar energy input during the flare. This ratio, shown as the yellow line in Figure 3 is plotted as a function of energy converted into wavelength with a 20 eV offset subtracted to approximate the average loss due to ionization energy. The peaks near 2 and 12 nm are morphologically consistent with the SEE observations and the flare model predictions. The collisional cascade of photoelectrons to lower energy lowers the peaks and fills the valleys for the photoelectron ratio, and increases the photoelectron flux towards lower energy (longer wavelengths). This trend in the photoelectron ratio is consistent with the measured solar EUV irradiance. Interestingly, the 2 nm peak in the photoelectron ratio is consistent with the estimated peak from the SEE XPS measurements but is at a slightly longer wavelength than the peak

predicted by the NRLEUV model near 1 nm. The 12 nm peak in the photoelectron ratio is also in reasonable agreement with the location of the second peak in the NRLEUV flare model ratio.

PHOTOELECTRON MODELING

Photoelectron fluxes were calculated using the GLOW model [*Solomon et al.,* 1988; *Solomon and Abreu*, 1989; *Bailey et al*., 2002] with the solar spectral irradiance measurements from SEE described above as inputs. The MSIS-86 thermospheric model [*Hedin*, 1987] is used to specify the neutral atmosphere. The model calculates photoionization, photodissociation, and excitation rates throughout the thermosphere, and generates a primary photoelectron spectrum. Photoelectron transport, including all cascade and secondary ionization processes, is computed using the two-stream approximation [*Nagy and Banks*, 1970]. The K-shell ionization and the resulting Auger electron production, which are important for comparison to the FAST photoelectron measurements, are included in the model. The upper boundary altitude employed for these runs was extended to 1000 km. The solar spectrum bin size is 0.1 nm at wavelengths from 0.1 to 30 nm to capture the details of the high-energy photoelectron spectrum, and 1 nm from 30 to 105 nm.

The upward fluxes calculated at 1000 km are simply extended to the satellite altitude of ~3700 km without attenuation, neglecting any effects on the escaping flux as it transits the plasmasphere. As confirmation that this approximation is valid, photoelectron calculations were performed using the FLIP model [Richards, 2002]. The FLIP model computes photoelectron fluxes up to 100 eV, but its altitude range extends through the plasmasphere. These results show that photoelectrons with energy 20 eV and higher have very similar fluxes at 1000 and 3700 km because the attenuation of the upflowing flux by Coulomb scattering reduces the flux by less than 20%. Most of this reduction consists of smoothing out the peaks in the photoelectron spectrum; at higher energies, where the flare enhancement is largest, changes in the photoelectron spectrum above 1000 km are insignificant [*P. Richards*, 2003, private communication].

Another source of uncertainty is that because the GLOW model uses the two-stream approximation, it does not provide the pitch-angle distribution of the photoelectrons. In order to compare with the FAST data we assume that the upward flowing (escaping) photoelectrons do not have a dependence on pitch angle. This approximation is accurate to within about 25% for energies greater than 40 eV [*Oran and Strickland*, 1978].

To obtain the best correspondence to the time of the FAST measurements, the SEE solar measurements are interpolated using logarithmic intensity to the times of the FAST flare measurement, about 20 minutes after SEE's first flare measurement. This solar spectrum is then input to the GLOW model, and the resulting photoelectron spectrum convolved with the FAST instrument response function. The comparison, shown in Figure 4, obtains reasonable agreement with the measured photoelectron distribution for both the pre-flare and during-flare cases. This agreement supports the higher solar XUV irradiance values reported by SNOE [*Bailey et al.*, 2000; 2001] and shown to be consistent with electron density profile and earlier photoelectron measurements [*Solomon et al.*, 2001].

There are some differences between the photoelectron measurements and models that are indicative of measurement and model uncertainties. The model slightly underestimates the preflare photoelectron flux at all energies, and the model slightly overestimates the flare photoelectron flux above 100 eV. These differences are well within the measurement and model uncertainties. The subtraction of the photoelectron background and its calibration uncertainty contribute about 40% uncertainty to the photoelectron measurements. The SEE solar measurements have a nominal uncertainty of about 15%. However, the spectral distribution within the bandpasses of the XPS measurements shortward of 27 nm is not known well because the XPS only has ~7 nm resolution. This results in uncertainties in the solar spectral irradiance shortward of 27 nm as high as ~30%. Considering these measurement uncertainties alone, the agreement between the GLOW model and photoelectron measurement is very good.

CONCLUSIONS

The measured solar EUV irradiance variations for the April 21 flare are similar as the predictions for the Bastille Day 2000 flare using the NRLEUV model. It is not clear whether these flare spectra are typical for large flares. Many additional smaller flares and a few more large X-class flares were observed by SEE during the TIMED mission, so the detailed analysis of these other flares should provide a better understanding of the changes in the EUV irradiances during flares.

The response of the photoelectrons to the flare event is a dramatic increase of the Auger electron fluxes. These high-energy electrons cascade to lower energy through collisions with the neutral atmosphere and thus provide a significant increase in energy for the ionosphere and neutral part of the mesosphere and surrounding layers. Initial modeling of the photoelectron distribution using the SEE measurements indicates reasonable agreement, but more de-

tailed analysis is planned for these flare data and other photoelectron data from FAST throughout the TIMED mission.

The absolute magnitude of the solar EUV irradiances has not been addressed here. The comparison between SEE and NRLEUV model predictions, as shown in Figure 3, indicate that the SEE measurements are higher by about a factor of 2 shortward of 27 nm but are in much better agreement at the longer wavelengths. Support for the higher solar XUV irradiance is provided by the results from modeling the photoelectron distribution, i.e., the results from the GLOW model using the SEE measurements as input are consistent with the photoelectron measurements. While the preliminary studies are encouraging for understanding the solar and photoelectron measurements, a thorough investigation is needed to fully validate them.

Finally, the effects of the solar flare extend beyond the photoelectrons to include effects on the composition, temperature, and dynamics of both the ionosphere and neutral atmosphere. As other data become available, the April storm period can serve as a test of our understanding of the atmosphere and its responses to sudden solar changes.

Acknowledgments. This work has been supported by NASA grant NAG5-11408 at the University of Colorado and by NASA grant NAG5-12449 to the University of Alaska.

REFERENCES

Bailey, S. M., T. N. Woods, C. A. Barth, S. C. Solomon, L. R. Canfield, and R. Korde, Measurements of the solar soft X-ray irradiance from the Student Nitric Oxide Explorer: first analysis and underflight calibrations, J. Geophys. Res., 105, *27179, 2000.*

Bailey, S. M., T. N. Woods, C. A. Barth, S. C. Solomon, L. R. Canfield, and R. Korde, Correction to "Measurements of the solar soft X-ray irradiance from the Student Nitric Oxide Explorer: first analysis and underflight calibrations", J. Geophys. Res., 106, *15791, 2001.*

Bailey, S. M., C. A. Barth, and S. C. Solomon, A model of nitric oxide in the thermosphere, J. Geophys. Res., in press. *2002.*

Brekke, P., G. J. Rottman, J. Fontenla, and P. G. Judge, The ultraviolet spectrum of a 3B class flare observed with SOLSTICE, Astrophys. J., 468*, 418, 1996.*

Carlson, C. W., J. P. McFadden, P. Turin, D. W. Curtis, and A. Magoncelli, The electron and ion plasma experiment for FAST, Space Sci. Rev., 98*, 33, 2001.*

Eparvier, F. G., T. N. Woods, G. Ucker, and D. L. Woodraska, TIMED Solar EUV Experiment: pre-flight calibration results for the EUV Grating Spectrograph, SPIE Proceedings, 4498, *91, 2001.*

Garcia, H., Thermal-spatial analysis of medium and large solar flares, 1976 to 1996, Ap. J. Suppl., 127*, 189, 2000.*

Garcia, H., Temperature and emission measure from GOES soft X-ray measurements, Solar Phys., 154*, 275, 1994.*

Handy, B. N. and 47 co-authors, The Transition Region And Coronal Explorer, Solar Phys., 187*, 229, 1999.*

Hedin, A. E., MSIS-86 thermospheric model, J. Geophys. Res., 92*, 4649, 1987.*

Lee, J. S., J. P. Doering, T. A. Potemra, and L. H. Brace, Measurements of the ambient photoelectron spectrum from Atmosphere Explorer, 1, AE-E measurements below 300 km during solar minimum conditions, Planet. Space. Sci, 28*, 947, 1980.*

Meier, R. R., H. P. Warren, A. C. Nicholas, J. Bishop, J. D. Huba, D. P. Drob, J. Lean, J. M. Picone, J. T. Mariska, G. Joyce, D. L. Judge, S. E. Thonnard, K. F. Dymond, and S. A. Budzien, Ionospheric and dayglow effects caused by the radiative phase of the Bastille Day flare, Geophys. Res. Lett*., 29, 99-1, 2002.*

Nagy, A. F., and P. M. Banks, Photoelectron fluxes in the ionosphere, J. Geophys. Res*., 75, 6260, 1970.*

Oran E. S. and D. J. Strickland, Photoelectron flux in the Earth's ionosphere, Planet. Space Sci*., **26**, 1161, 1978.*

Peterson, W. K., J. P. Doering, T. A. Potemra, R. W. McEntire, and C. O. Bostrom Conjugate photoelectron fluxes observed on Atmosphere Explorer C, Geophys. Res. Lett,. 4*, 109, 1977.*

Richards, P. G., Ion and neutral density variations during ionospheric storms in September 1974: Comparisons of measurement and models, J. Geophys. Res*.,* 107*, 10, 2002.*

Solomon, S. C. and V. J. Abreu, The 630 nm dayglow, J. Geophys. Res., 94*, 6817, 1989.*

Solomon, S. C., P. B. Hays, and V. J. Abreu, The auroral 6300 Å emission: Observations and modeling, J. Geophys. Res., 93*, 9867, 1988.*

Solomon, S. C., S. M. Bailey, and T. N. Woods, Effect of solar soft X-rays on the lower ionosphere, Geophys. Res. Lett., 28*, 2149, 2001.*

Warren, H. P., J. T. Mariska, and J. Lean, A new model of solar EUV irradiance variability. 1. Model Formulation, J. Geophys. Res., 106*, 15745, 2001.*

Winningham, J. D. D. T. Decker, J. U. Kozyra, J. R. Jasperse, and A. F. Nagy, Energetic (>60 eV) atmospheric photoelectrons, J. Geophys. Res., 904*, 15335, 1989.*

Woods, T., F. Eparvier, S. Bailey, S. C. Solomon, G. Rottman, G. Lawrence, R. Roble, O. R. White, J. Lean, and W. K. Tobiska, TIMED Solar EUV Experiment, SPIE Proceedings, 3442*, 180, 1998.*

Woods, T., E. Rodgers, S. Bailey, F. Eparvier, and G. Ucker, TIMED Solar EUV Experiment: pre-flight calibration results for the XUV Photometer System, SPIE Proceedings, 3756, *255, 1999.*

Woods, T. N. and 13 co-authors, Solar extreme ultraviolet and X-ray irradiance variations, in Solar Variability and Its Effect on Earth's Atmospheric and Climate System*, ed. J. Pap, C. Frohlich, H. Hudson, J. Kuhn, J. McCormack, G. North, W. Spring, and S. T. Wu., AGU Monograph, Washington, DC, in press, 2003.*

Thomas N. Woods, William K. Peterson, and Francis G. Eparvier, Laboratory for Atmospheric and Space Physics, University of Colorado, 1234 Innovation Dr., Boulder, CO 80303

Scott M. Bailey, University of Alaska, 903 Koyukuk Dr., Fairbanks, AK 99775-7320

Harry P. Warren, Naval Research Laboratory, 4555 Overlook Ave. S.W., Washington, DC 20375-5000

Stanley C. Solomon, National Center for Atmospheric Research, 3450 Mitchell Lane, Boulder, CO 80301

Howard Garcia, NOAA Space Environment Center, 325 Broadway, Boulder, CO 80303

Charles W. Carlson and James P. McFadden, Space Sciences Laboratory, University of California at Berkeley, Berkeley, CA 94720